ISSN: 2449 - 0539
BAYERO JOURNAL OF ENGINEERING AND TECHNOLOGY VOL. 18 NO. 2 MAY 2023 PP. 84-94

A STUDY OF MOTOR SENSITIVITY TO PARAMETERS VARIATION IN EXTERIOR PERMANENT MAGNET SYNCHRONOUS MOTOR

Ezeonye, C.S[1*], Onwuka, I.K[2], Oputa, O[2], and Obi, P.I[2]

[1] Department of Electrical & Electronic Engineering, University of Agriculture and Environmental Sciences, Umuagwo, Imo State, Nigeria.
[2] Department of Electrical & Electronic Engineering, Michael Okpara University of Agriculture, Umudike, Abia state, Nigeria.
Email: ezeonyechinonso@yahoo.com*, onwuka.ifeanyichukwu@mouau.edu.ng, connectositao@gmail.com, patndyobi@gmail.com

ABSTRACT

This paper presents the study of motor sensitivity to parameters variation on the dynamic behaviour of exterior permanent magnet synchronous motor with the aid of matlab m-file for simulation. This study is carried out due to factors that hinder the motor performance like limited speed range and high stator core loss. The motor differential models are indicated in reference frame of the rotor with rotor angular position, mechanical rotor speed, q- and d-axes stator currents as state variables. The motor parameters used in this research is a 3-phase, 2 KW, 50 Hz, 4 poles, 220 V. The results showed that increase in frequency leads to increase in motor synchronous speed (1500 rpm to 2250 rpm to 3000 rpm for 50 Hz, 75 Hz and 100 Hz respectively) due to its direct relation, and slightly increased electromagnetic torque and output power. The frequency variation helps in determining the motor speed range. The effect of increase in resistance of the stator winding shows that it reduces the magnitude of ripple of the output characteristics (torque, power and speed) but maintains the same steady state value, while the effect of increase in coefficient of viscous friction decreases the magnitude of ripple and increase the value of the steady state. Similarly, variation on the inertia moment of the motor has little or no effect on the motor output characteristics. Effect of load variation only affects the output power and air-gap torque of the motor as increase or decrease in load leads to increase or decrease in output power and air-gap torque respectively. The loading of the motor is not to exceed the 15 Nm otherwise, the motor will operate in reverse condition. The results gotten in this research as compared to other literatures gives a clear understanding and knowledge of the parameters required of a particular motor for improve operating performance with respect to the design requirement.

Keywords: Electromagnetic torque; Electromechanical power; Exterior permanent magnet synchronous motor (EPMSM); Permanent magnet (PM); Synchronous speed

1. INTRODUCTION

Exterior permanent magnet synchronous motors (EPMSM) play a very important role in the industry due to its negligible rotor loss, high efficiency, absence of external source of magnetization current for excitation, smaller in size and lesser weight (Ichikawa *et al*., 2006; Jacek, 2017). It is a type of motor that is incorporated with a permanent magnet used in producing air gap flux rather than the electromagnets that is applied in conventional motors (Ukoima *et al*., 2019; Ukoima *et al*., 2020; Obi *et al*., 2022). The motor stator is designed with three-phase winding connected to alternating current (AC) supply while the magnet is connected to the rotor circuit (Siva *et al.,* 2013; Shady, 2016). The importance of parameters variation and sensitivity in EPMSM stems from the need to achieve the motor improved operating performance (Babel *et al*., 2012; Onwuka *et al*., 2023).

The exterior PMSM of Figure 1 configuration has magnets magnetized radially or circumferentially. An external cylinder containing non-ferromagnetic material is sometimes used (Arroyo, 2006). It protects the permanent magnets against damage due to centrifugal forces, the demagnetizing action of the armature reaction provides an asynchronous starting torque and acts as a damper. It can be applied in speed range of about 3000 rpm or below because of the possibility that magnets will fly apart during high-speed operations. The effective air gap of the *d*-axis equals that of the *q*-axis and the motors are considered to have small or no saliency, thus having practically equal inductances in both axes ($L_d = L_q$) and torque is produced by the interaction between the stator currents and the magnets only. It has low permanent magnet flux leakage, small armature reaction flux, poor flux-weakening (Krishnan, 2001; Bose, 2002; Liu, 2005; Alexander, 2006).

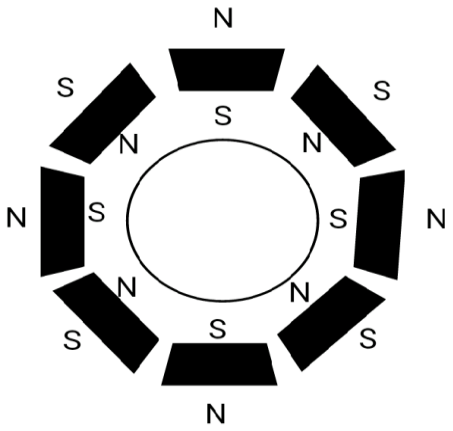

Figure 1: Exterior permanent magnet

A review and analysis of parameter measurements for PMSM was presented by Kondo (2007). The reviews show how electrical and mechanical parameters of PMSM can be measured but the parameters estimation and measurement effect on the output speed, torque and power of the motor was not shown. Performance operation of the PM motor speed with application of varied load was presented by Siva *et al.* (2013) with the aid of Simulink. However, the effect of variation of other output parameters to the motor speed was not shown. Estimation of PMSM magnetic saliency with the aid of measurement method and injection technique was presented by Brandstetter and Krecek (2014). Estimation of parameters of PMSM using matlab/simulink for the simulation was reviewed by Ramana *et al.* (2015). The electrical parameters are evaluated by off-line as well as on-line techniques but mechanical parameters are assessed by on-line methods only. The results showed that the system maintains stability in 40 Hz to 50 Hz frequency range. However, the effect of other parameters to the performance of motor was not depicted. Saliency and core loss effect on interior and surface PMSM was analyzed by Ezeonye *et al*. (2020) in which speed, air-gap torque and mechanical output power was considered as one of the motor characteristics, but the effect of increase and decrease in motor parameters which affect its sensitivity was not considered. In analysis and simulation of interior PMSM presented by Ezeonye *et al*. (2022), observations were made when the connected load to the motor is varied intermittently. This variation was proved to affects the motor operation when it is loaded beyond it carrying capacity. However, the effect of increase or decrease in output parameters of the motor like core resistance, inertia constant and viscous friction which considerably affect the motor dynamic operation was not done.

From the literatures reviewed, the sensitivity of PMSM parameters such as the coefficient of viscous friction, inertia moment of the motor, stator resistance, and frequency was not carried out in their analysis. As a result, a study of the mentioned parameters variation is carried out in this work. This is done in order to determine the sensitivity of these parameters to the operation of exterior PMSM for proper selection of their values during the design of the motor.

2. MATERIALS AND METHOD

The materials used in carrying out this research are exterior PMSM model of 2 KW, 2.68 HP, 220V, 50 Hz, Matlab/Simulink R2015a software, HP window 8, 4GB installed memory, 64-bit operating system laptop. Matlab m-file was employed in modeling and simulation of exterior PMSM to observe its behaviour under the conditions of variations and sensitivity of the parameters. The motor model has been developed in reference frame of the rotor as shown in Figure 2 by assuming that saturation is neglected, induced electromotive force is sinusoidal, eddy currents and hysteresis losses are neglected, and there are no field current dynamics (Ezeonye *et al*., 2022).

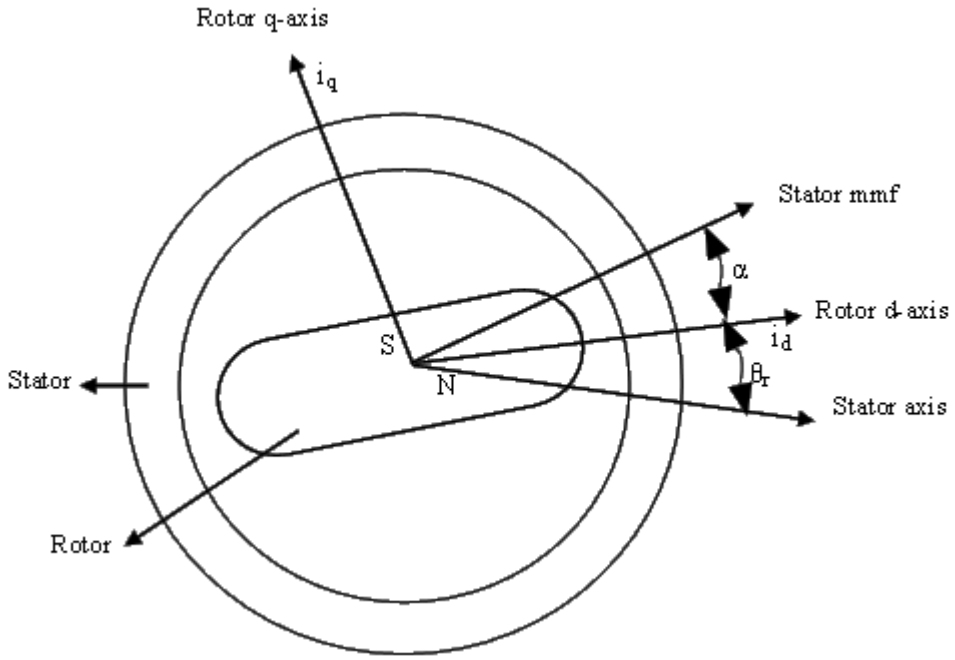

Figure 2: Axis of the exterior permanent magnet motor

2.1 Exterior PMSM Model

The equivalent circuit of the exterior PMSM is shown in Figure 3. The model equations, the voltage, current and flux linkage, of the motor as depicted in Equations 1 to 12 (El Shewy *et al.,* 2008; El Shahat and El Shewy, 2010).

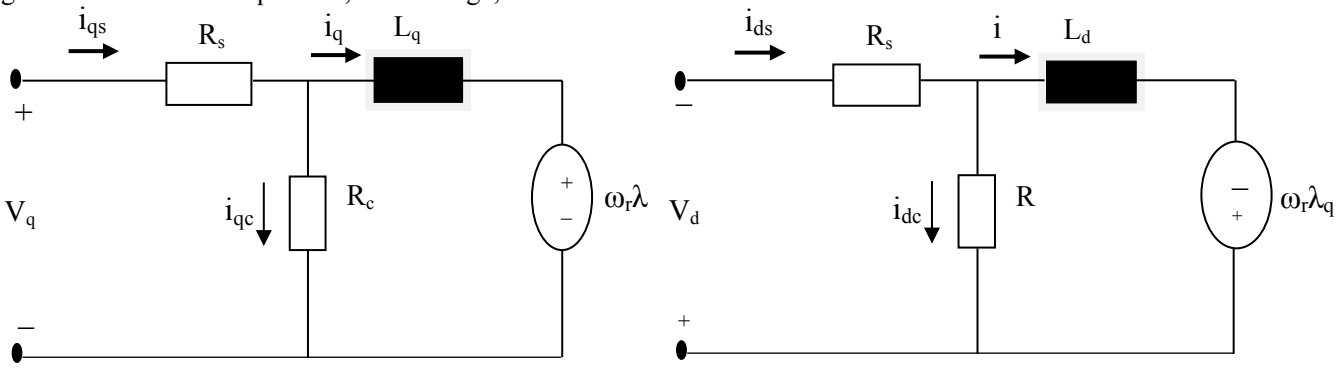

Figure 3: Equivalent circuit of EPMSM

The axis voltage equations can be expressed as:

$$V_q = R_s i_q + \frac{(R_s+R_c)}{R_c}\rho(\lambda_q) + \frac{(R_s+R_c)}{R_c}\omega_r\lambda_d \quad (1)$$

$$V_d = R_s i_d + \frac{(R_s+R_c)}{R_c}\rho(\lambda_d) - \frac{(R_s+R_c)}{R_c}\omega_r\lambda_q \quad (2)$$

Where the axis flux linkages in the rotor reference frame are

$$\lambda_q = L_q i_q \quad (3)$$

$$\lambda_d = L_d i_d + \lambda_m \quad (4)$$

When Equations (3) and (4) are substituted in Equations (1) and (2), it gives

$$V_q = R_s i_q + \frac{(R_s+R_c)}{R_c}\rho(L_q i_q) + \frac{(R_s+R_c)}{R_c}\omega_r(L_d i_d + \lambda_m) \quad (5)$$

$$\frac{di_q}{dt} = \frac{-R_s R_c}{L_q(R_s+R_c)} i_q - \frac{\omega_r L_d}{L_q} i_d + \frac{V_q R_c}{L_q(R_s+R_c)} - \frac{\omega_r\lambda_m}{L_q} \quad (6)$$

$$V_d = R_s i_d + \frac{(R_s+R_c)}{R_c}\rho(L_d i_d + \lambda_m) - \frac{(R_s+R_c)}{R_c}\omega_r L_q i_q \quad (7)$$

$$\frac{di_d}{dt} = \frac{\omega_r L_q}{L_d} i_q - \frac{R_s R_c}{L_d(R_s+R_c)} i_d + \frac{V_d R_c}{L_d(R_s+R_c)} \quad (8)$$

Where

ρ: Operator $\frac{d}{dt}$

$\rho(\lambda_m) = 0$
V_q and V_d: q- and d-axis voltages
i_q and i_d: q- and d-axis currents
L_q and L_d: q- and d-axis inductances
λ_q and λ_d: q- and d-axis flux linkages
R_s: Stator resistance
R_c: Core resistance
ω_r: Electrical speed of the rotor
λ_m: Rotor flux linkage.
The general mechanical equation for the motor is given as:

$$T_e = T_l + T_d + B\omega_{rm} + J\rho\omega_{rm} \quad (9)$$

Electromagnetic torque of the motor in terms of d- and q-axis flux linkages, rotor flux linkage, and d- and q-axis inductances is given as:

$$T_e = \frac{3}{2}\left(\frac{P}{2}\right)\left(\lambda_d i_q - \lambda_q i_d\right) \quad (10)$$

Substituting Equations (3) and (4) into Equation (10) gives

$$T_e = \frac{3}{2}\left(\frac{P}{2}\right)\left(\lambda_m i_q + \left(L_d - L_q\right) i_q i_d\right) \quad (11)$$

Solving for the rotor mechanical speed from Equation (9), assuming the dry friction is equals zero gives

$$\frac{d}{dt}\begin{bmatrix} i_q \\ i_d \\ \omega_{rm} \\ \theta_r \end{bmatrix} = \begin{bmatrix} \frac{-R_s R_c}{L_q(R_s+R_c)} & \frac{-\omega_r L_d}{L_q} & 0 & 0 \\ \frac{\omega_r L_q}{L_d} & \frac{-R_s R_c}{L_d(R_s+R_c)} & 0 & 0 \\ 0 & 0 & \frac{-B}{J} & 0 \\ 0 & 0 & 0 & 0 \end{bmatrix}\begin{bmatrix} i_q \\ i_d \\ \omega_{rm} \\ \theta_r \end{bmatrix} + \begin{bmatrix} \frac{1}{L_q}\left(\frac{V_q R_c}{R_s+R_c} - \omega_r\lambda_m\right) \\ \frac{V_d R_c}{L_d(R_s+R_c)} \\ \frac{1}{J}(T_e - T_l) \\ \omega_r \end{bmatrix} \quad (17)$$

The dynamic dq equations are applied in the analysis of EPMSM during steady and transient state operations. This is done by changing the three-phase voltages and currents to dq variables by the application of Park's transformation method (Krause *et al*., 2013).

The reference frame voltages of EPMSM under the condition of balance state can be estimated as:

$$V_a = \sqrt{2}V\cos\omega_b t \quad (18)$$

$$V_b = \sqrt{2}V\cos(\omega_b t - \frac{2\pi}{3}) \quad (19)$$

$$V_c = \sqrt{2}V\cos(\omega_b t + \frac{2\pi}{3}) \quad (20)$$

where

$$\frac{d\omega_{rm}}{dt} = \frac{-B}{J}\omega_{rm} + \frac{1}{J}(T_e - T_l) \quad (12)$$

also

$$\frac{d\theta_r}{dt} = \omega_r \quad (13)$$

The electromechanical power is given as:

$$P_{em} = \omega_{rm}T_e = \frac{3}{2}\omega_r\left(\lambda_d i_q - \lambda_q i_d\right) \quad (14)$$

$$\omega_r = \frac{P}{2}\omega_{rm} \quad (15)$$

The mechanical speed N (that is synchronous speed) in terms of revolutions per minute (rpm) can be stated as

$$N = \frac{30}{\pi} \times \omega_{rm} \quad (16)$$

Where:
P: Number of poles
ω_{rm}: Mechanical velocity of the rotor
B: Viscous frictions coefficient
J: Inertia of the shaft and the load system
T_d: Dry friction
T_l: Load torque
T_e: Electromagnetic torque
θ_r: Electrical Rotor angular position
N: Synchronous speed
Combining Equations (6), (8), (12), and (13) in state variable form gives
$\omega_b = 2\pi f$ is the rated source frequency in rad/s
V_a, V_b, and V_c: Stator phase a, b, c voltages
V: Line voltage

The three-phase voltages of the stator circuit are related to q- and d-axis reference frame as follows:

$$\begin{bmatrix} V_q \\ V_d \end{bmatrix} = \frac{2}{3}\begin{bmatrix} cos\theta & cos(\theta-120) & cos(\theta+120) \\ sin\theta & sin(\theta-120) & sin(\theta+120) \end{bmatrix}\begin{bmatrix} V_a \\ V_b \\ V_c \end{bmatrix} \quad (21)$$

$$\begin{bmatrix} V_a \\ V_b \\ V_c \end{bmatrix} = \begin{bmatrix} cos\theta & sin\theta \\ cos(\theta-120) & sin(\theta-120) \\ cos(\theta+120) & sin(\theta+120) \end{bmatrix}\begin{bmatrix} V_q \\ V_d \end{bmatrix} \quad (22)$$

Likewise, the three phase currents can be evaluated in the same way as:

$$\begin{bmatrix} i_q \\ i_d \end{bmatrix} = \frac{2}{3}\begin{bmatrix} cos\theta & cos(\theta-120) & cos(\theta+120) \\ sin\theta & sin(\theta-120) & sin(\theta+120) \end{bmatrix}\begin{bmatrix} i_a \\ i_b \\ i_c \end{bmatrix} \quad (23)$$

$$\begin{bmatrix} i_a \\ i_b \\ i_c \end{bmatrix} = \begin{bmatrix} cos\theta & sin\theta \\ cos(\theta-120) & sin(\theta-120) \\ cos(\theta+120) & sin(\theta+120) \end{bmatrix}\begin{bmatrix} i_q \\ i_d \end{bmatrix} \quad (24)$$

Where i_a, i_b, and i_c are stator phase a, b, c currents while θ is the phase angle.

3. RESULTS AND DISCUSSION

The motor comprehensive parameters selected in the simulation performance using matlab m-file is as shown in Table 1. The observations of the motor operation are shown in the results.

Table 1: Parameters for exterior permanent magnet synchronous motor

Motor Parameter	Value
Rated power, P	2 kW
Rated voltage, V	220 V
Rated speed, ω	1500 rpm
q-axis inductance, L_q	0.0170 H
d-axis inductance, L_d	0.0170 H
Rotor flux linkage, λ_{af}	0.320 Wb
Number of poles, P	4
Stator resistance, R_s	5.28 Ω
Stator core resistance, R_c	18 Ω
Inertia coefficient, J	0.00020 kg/m^2
Load torque, T_l	10 Nm
Dry friction, T_d	0 Nm
Frequency, f	50 Hz
Viscous friction coefficient, B	0.014 Nms

Figures 4 to 8 show the effect of varying parameters on electromagnetic torque of EPMSM. As stator resistance is decreased to half of the given value, the magnitude of the torque ripple increases while the ripple decreases when the resistance is increased beyond 5.28 ohms as can be seen in Figure 4. Figure 5 shows that decrease in inertia coefficient gives less distortion and takes less time to attain its steady state as compared to its higher values. As viscous friction is decreased, the steady state value of electromagnetic torque is decreased from 3 Nm to 2 Nm and to 1 Nm as seen in Figure 6. From Figure 7, it is seen that increase in frequency increases the magnitude of the steady state value of the electromagnetic torque. Figure 8 shows that variation of load directly affects air-gap torque due to its direct proportion as explained in the models. However, when the motor is loaded beyond 200% of 10 Nm, it goes out of synchronism. This indicates that the motor with parameters as given in Table 1 cannot be loaded beyond that level.

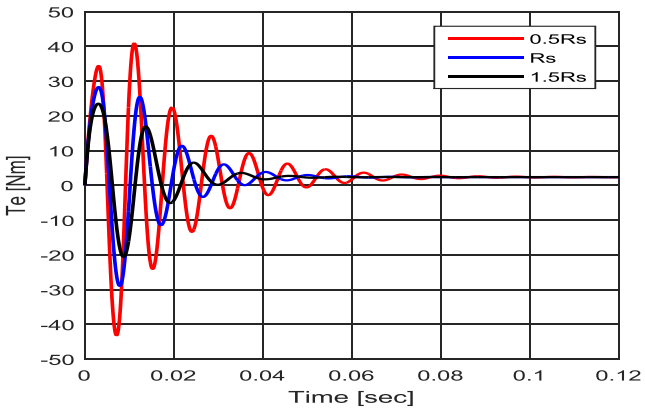

Figure 4: Air-gap torque response for variable stator resistance

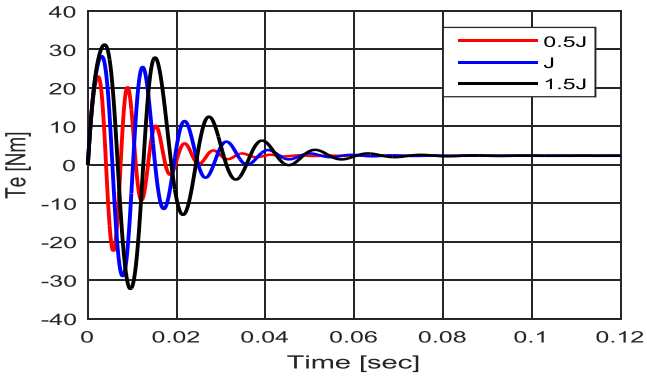

Figure 5: Air-gap torque response for variable inertia coefficient

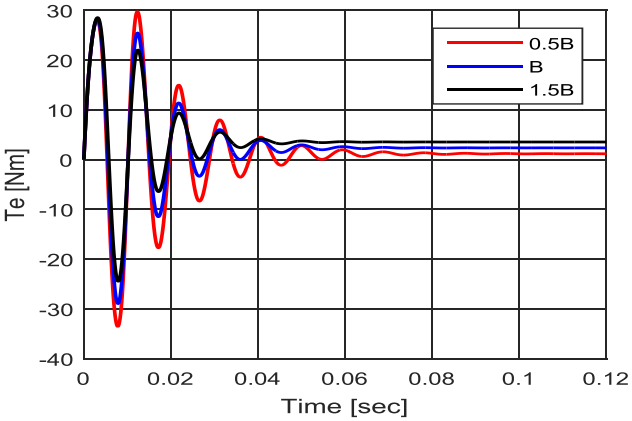

Figure 6: Air-gap torque response for variable viscous friction

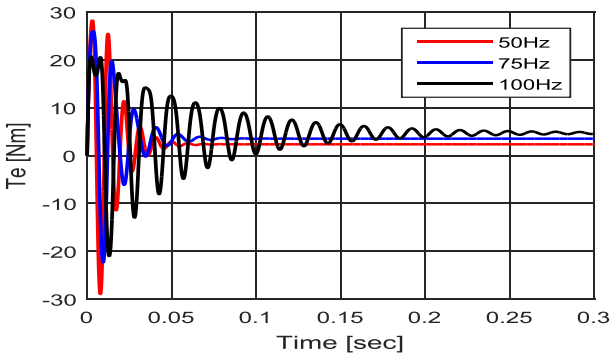

Figure 7: Air-gap torque response for variable frequency

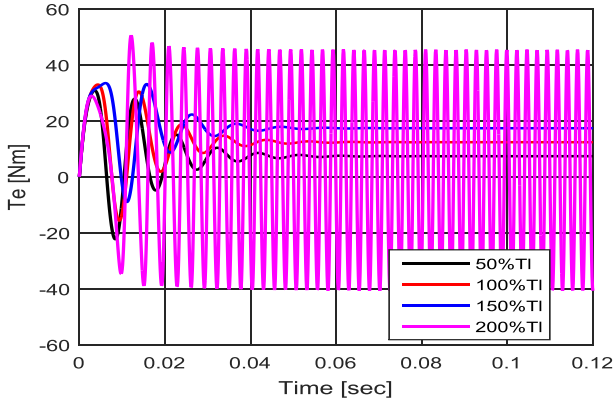

Figure 8: Air-gap torque response for varied load

Figures 9 to 13 show the effect of varying parameters on mechanical output power of EPMSM. As stator resistance is decreased, the magnitude of the ripple of the output power increases and it takes more time to attain its steady state, but the steady state of the electromechanical power remains the same at 0.5 kw irrespective of the variation in stator resistance. Figure 10 shows that decrease in inertia moment gives less distortion and takes less time to attain its steady state. Also, as viscous friction coefficient is decreased to half of the given value, the output power is decreased to 0.25 kw and it introduces more ripples. It is seen from Figure 12 that as frequency is increased, electromechanical output power increases from 0.5 kw to 1.0 kw to 1.5 kw respectively since it has direct relation with torque. Also, Figure 13 shows that increase in load increases the output power but it is to be noted that the load will not exceed 1.5 of its rated value, otherwise there will be fluctuation in the output.

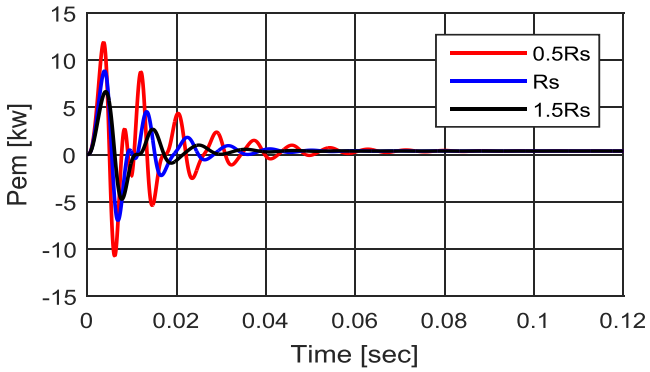

Figure 9: Output power response for variable stator resistance

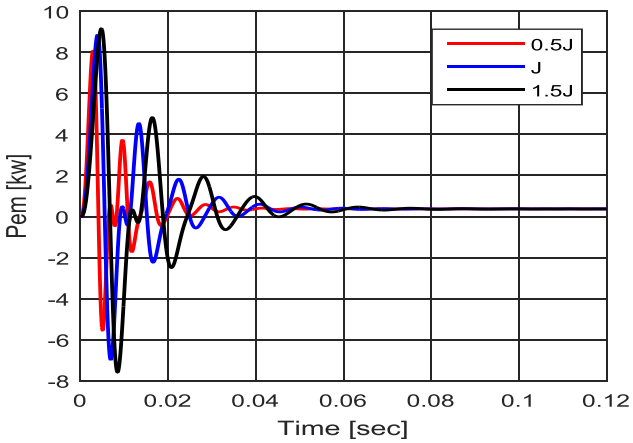

Figure 10: Output power response for variable inertia coefficient

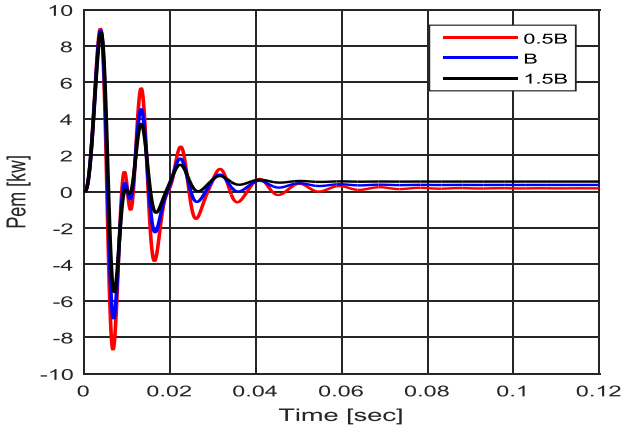

Figure 11: Output power response for variable viscous friction

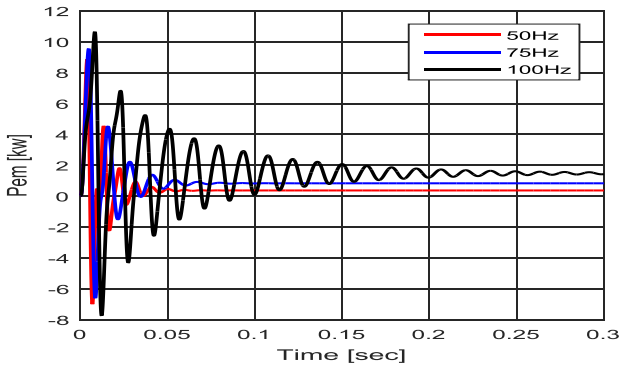

Figure 12: Output power response for variable frequency

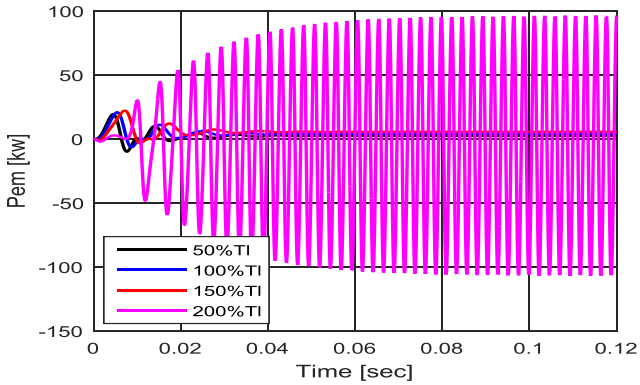

Figure 13: Output power response for load variation

Figures 14 to 18 show the effect of varying parameters on synchronous speed of exterior PMSM. It is seen from Figure 14 that as stator resistance is varied, the steady state speed of the rotor remains constant at 1500 rpm. The only effect of decreasing stator resistance is that it introduces more ripples and takes more time to settle. Also Figure 15 shows that the speed of the rotor remains constant with variation of its inertia, and the magnitude of the ripples varies slightly. In the same vein, Figure 16 shows that as viscous friction coefficient is varied, the speed of the rotor remains constant. The only effect of decreasing viscous friction coefficient is that it introduces higher ripples of 4250 rpm. It is seen from Figure 17 that increase in frequency from 50 Hz to 75 Hz to 100 Hz increases the magnitude of the steady state speed of the motor from 1500 rpm to 2250 rpm to 3000 rpm respectively, as speed is directly related to frequency of supply. It equally showed that when the frequency is at 100 Hz, it took more time to attain the steady state and further increase leads to unsynchronous operation of the motor. Figure 18 affirmed that on loading the motor to 200% of the rated load, the speed became unstable, hence for stability of speed, the motor operates optimally from 1.5 of the rated load torque and below as it maintained steady speed of 1500 rpm.

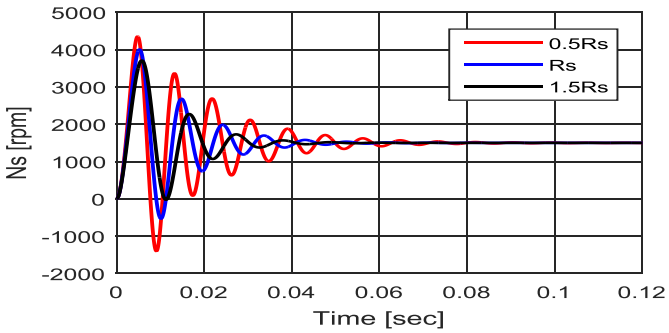

Figure 14: Synchronous speed response for variable stator resistance

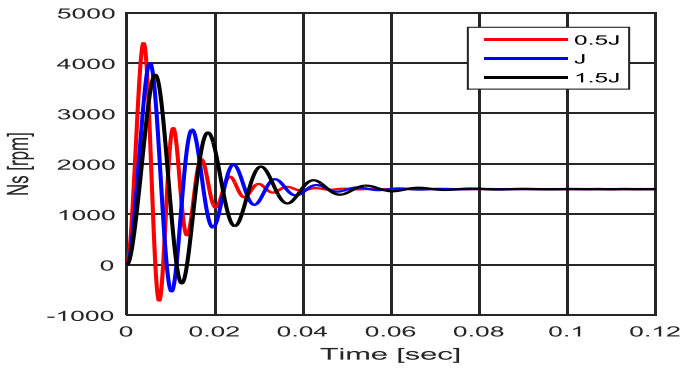

Figure 15: Synchronous speed response for variable inertia coefficient

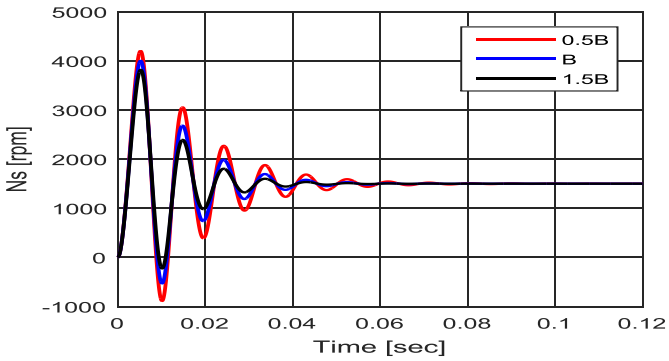

Figure 16: Synchronous speed response for variable viscous friction

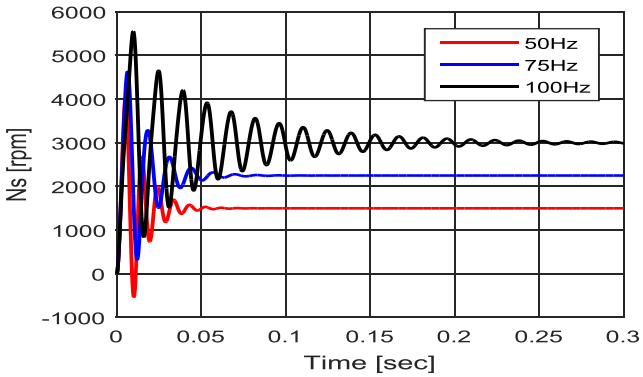

Figure 17: Synchronous speed response for variable frequency

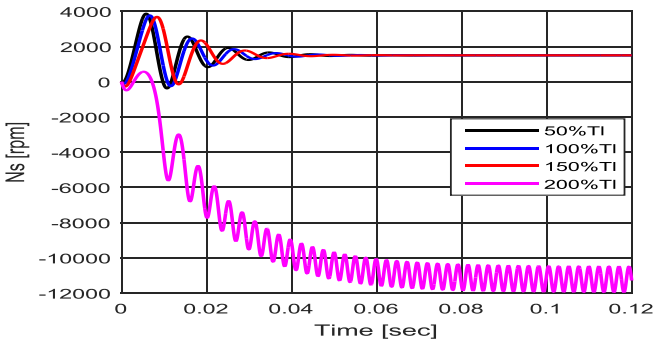

Figure 18: Synchronous speed response for variable load

The torque-speed characteristics of exterior PMSM is shown in Figures 19 to 22. The responses show that the run-up characteristics of the motor is highly cyclic. In Figure 19 to 22, the relationship between speed and torque of EPMSM irrespective of parameters variation shows that as value of stator resistance increases, it leads to greater value of slip at which the air gap torque is achieved. This implies that as the resistance is increased, the maximum torque remains constatnt. Figure 22 shows the speed-torque characteristics of EPMSM for 5 Nm, 10Nm, 15Nm, and 20 Nm. At the point of 20 Nm, the response of speed and torque does not correlate as the cyclic nature of the response was altered which also means unsynchronous operation of the motor.

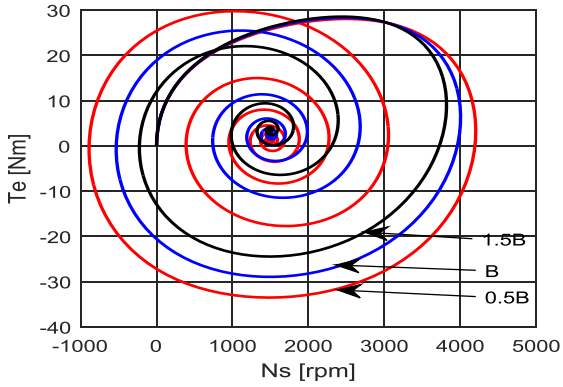

Figure 19: Speed torque response for variable viscous friction

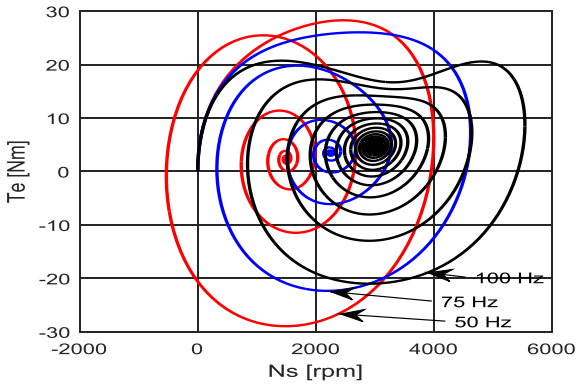

Figure 20: Speed torque response for variable frequency

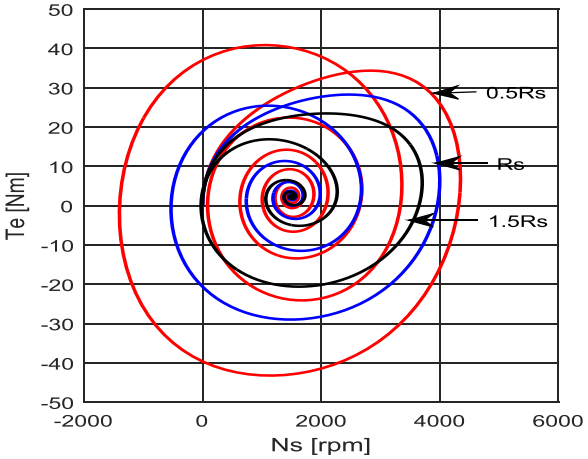

Figure 21: Speed torque response for variable stator resistance

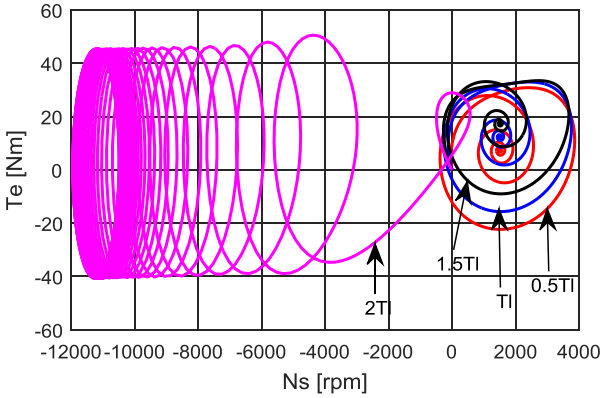

Figure 22: Speed torque response for variable load

Figure 23 and 24 show the effect of load variation on stator current response of EPMSM. In Figure 23, the response of i_a, i_b, and i_c were shown with respect to time. When load torque is decreased from 10 Nm to 5 Nm, it decreased the magnitude of the steady state stator current from 30 A to

29 A, but when it increased to 15 Nm, it increases the value of steady state as can be verily seen from Figure 24. This shows that stator current is minimum at no-load, and increases to attain rated current at rated load torque. It is worthy to note that on increase in load torque, more time is required for attainment of steady state as peak magnitude of ripple eclipsed to 40 Nm. However, when the load reaches 20 Nm, the current waveform became unstable and hence out of synchronism. This is depicted clearly in phase 'b' stator current waveform in Figure 24.

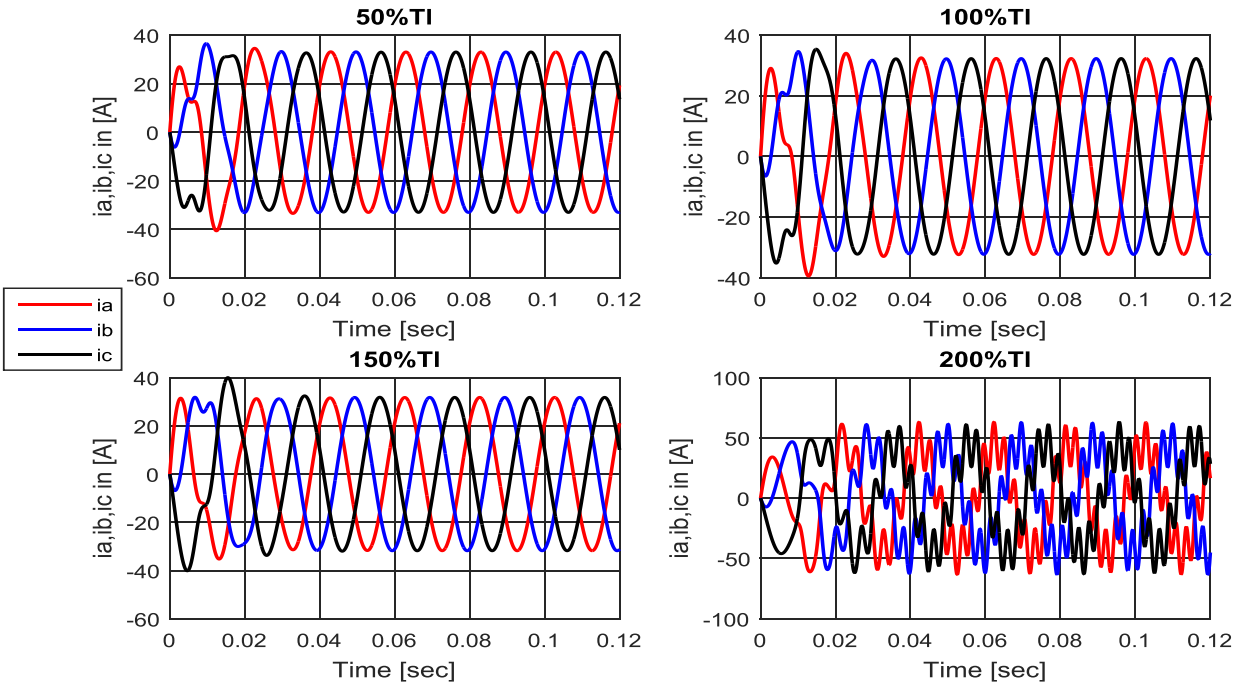

Figure 23: Stator current response for variable load

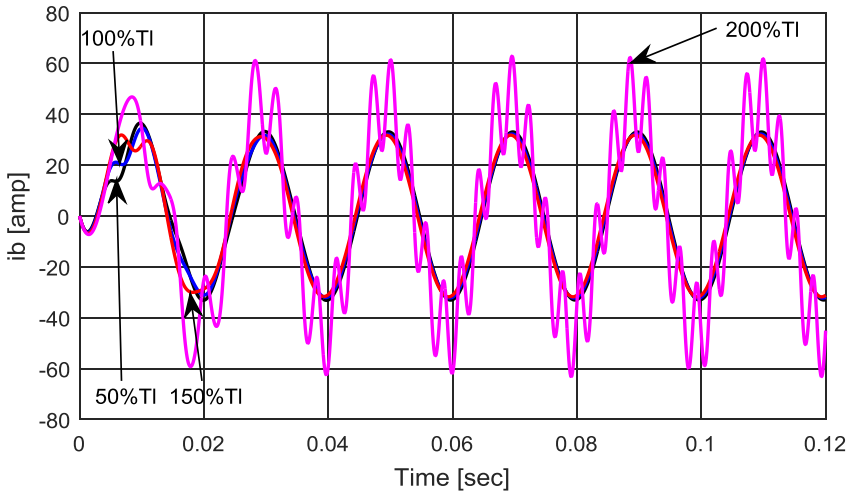

Figure 24: Phase 'b' stator current response for variable load

4. CONCLUSION

The simulation results show that the sensitivity of motor parameters such as stator resistance needs to be equal or higher than that given in Table i (Rs=5.28 Ω) since the lower value introduces higher ripples on the responses. Similarly, the inertia of the motor when decreased by 50% reduces the ripple magnitude of the motor parameters. Also, on the variation of viscous friction coefficient, when decreased by 50% with respect to the given value, the magnitude of the ripples of the output parameters of the motor increased slightly but this also helps in aligning the steady state values of electromagnetic torque to the values of load torque. The simulation results show that the speed as evaluated to determine the performance characteristics of the motor remain constant even with variation of load torque. The variation effect of load torque only affects the electromagnetic torque and electromechanical power of the motor due to their direct relations. The results established in this analysis as correlated to other researches show enhanced design of exterior PMSM with clear knowledge and perspective of the parameters required of a particular motor for improve operating performance. It is recommended that experimental implementation on the speed-torque response be carried out though the EPMSM has a good start-up performance and speed-torque response.

REFERENCES

Alexander, S. (2006). Design and Optimization of a Surface-Mounted Permanent Magnet Synchronous Motor for a High Cycle Industrial Cutter. *Master Thesis.* Department of Electrical Engineering, Electrical Machines and Power Electronics, Royal Institute of Technology, Stockholm, Sweden.

Arroyo, E. L. C. (2006). Modeling and Simulation of Permanent Magnet Synchronous Motor Drive System. *Thesis for Master of Science*. Electrical Engineering Department, University of Puerto Rico Mayaguez.

Babel, A. S., Foster, S. N., Cintron-Rivera, J. G. and Strangas, E. G. (2012). Parametric Sensitivity in the Analysis and Control of Permanent Magnet Synchronous Machines. *2012 XXth International Conference on Electrical Machines*, Marseille, France, 2-5 September, 2012, pp. 1034-1040.

Bose, B. K. (2002). *Modern Power Electronics and AC Drives*. Prentice Hall PTR, New Jersey, USA.

Brandstetter, P., and Krecek, T. (2014). Estimation of PMSM Magnetic Saliency using Injection Technique. *Journal of Elektronika Ir Elektrotechnika,* Vol. 20, No, 2, pp. 22-27.

El Shahat, A. and El Shewy, H. M. (2010). Permanent Magnet Synchronous Motor Dynamic Modeling with Genetic Algorithm Performance Improvement. *International Journal of Engineering, Science and Technology*, Vol. 2, No. 2, pp. 93-106.

El Shewy, H. M., Abd Al Kader, F. E., El Kholy, M. M. and El Shahat, A. (2008). Dynamic Modeling of Permanent Magnet Synchronous Motor using Matlab – Simulink. *6th International Conference on Electrical Engineering (ICEENG)*, Suez, Egypt, pp. 1-16.

Ezeonye, C. S., Nkan, I. E., Okpo, E. E. and Okoro, O. I. (2022). Dynamic Analysis and Computer Simulation of Interior Permanent Magnet Synchronous Motor with Intermittent Loading. *Nigerian Journal of Technology (NIJOTECH),* Vol. 41, No. 1, pp. 148-157.

Ezeonye, C. S., Okpo, E. E., Nkan, I. E., and Okoro, O. I. (2020). Effect of Saliency and Core Losses on the Dynamic Behavior of Permanent Magnet Synchronous Motor. *Bayero Journal of Engineering and Technology (BJET),* Vol. 15, No. 3, pp. 124-133.

Ichikawa, S., Tomita, M., Doki, S. and Okuma, S. (2006). Sensorless Control of Permanent-Magnet Synchronous Motors using Online Parameter Identification Based on System Identification Theory. *IEEE Transactions on Industrial Electronics*, Vol. 53, No. 2, pp. 363-372.

Jacek F. G. (2017). *Electrical Machines: Fundamentals of Electromechanical Energy Conversion*. CRC Press, Boca Raton, London, UK.

Kondo, M. (2007). Parameter Measurements for Permanent Magnet Synchronous Machines. *IEEJ Transactions on Electrical and Electronic Engineering*, Vol. 2, No. 2, pp. 109-117.

Krause, P., Wasynczuk, O., Sudhoff, S. and Pekarek, S. (2013). *Analysis of Electric Machinery and Drive Systems*. 3rd edition. John Wiley & Sons, Inc., New Jersey.

Krishnan, R. (2001). *Electric Motor Drives Modelling, Analysis and Control.* Prentice Hall Inc, Upper Saddle River, New Jersey, USA.

Liu, Q. (2005). Analysis, Design and Control of Permanent Magnet Synchronous Motors for Wide-Speed Operation. *Thesis for Doctor of Philosophy.* Department of Electrical Engineering, National university of Singapore.

Obi, P. I., Diyoke, G. C. and Onwuka, I. K. (2022). Determining Efficiency of Brushless Permanent Magnet DC Motor using Magnetic Circuit Simulation. *NIPES Journal of Science and Technology Research*, Vol. 4, No. 1, pp. 200-211.

Onwuka, I. K., Obi, P. I., Oputa, O. and Ezeonye, C. S. (2023). Performance Analysis of Induction Motor with Variable Air-Gaps using Finite Element Method. *NIPES Journal of Science and Technology Research*, Vol. 5, No. 1, pp. 112-124.

Ramana, P., Mary, K. A., Kalavathi, M. S., and Swathi, A. (2015). Parameter Estimation of Permanent Magnet Synchronous Motor – A Review. *I-manager's Journal on Electrical Engineering,* Vol. 9, No. 2, pp. 46-56.

Shady, M. S. A. (2016). Direct Torque Control of Permanent Magnet Synchronous Motors (DTC PMSM). *Thesis for Master of Science*. Electrical Power and Machines Engineering Department, Cairo University Giza, Egypt.

Siva, G. R. V., Sneha, V. and Sravani, M. (2013). Mathematical Modeling and Simulation of Permanent Magnet Synchronous Motor. *International Journal of Advanced Research in Electrical Electronics and Instrumentation Engineering*, Vol. 2, No. 8, pp. 3720-3726.

Ukoima, K. N., Ezeonye, C. S., Abara, I. E., and Chikere, N. C. (2020). A Study of the Effects of Proportional, Integral and Derivative Controller in the Speed Regulation of an Armature Controlled Direct Current Motor. *Journal of Control System and Control Instrumentation,* Vol. 6, No. 1, pp. 5-10.

Ukoima, K. N., Obi, P. I. and Ezeonye, C. S. (2019). Dynamic Modelling of Excitation and Governor Effect on Stability of Electrical Machines. *2nd International Engineering Conference, IECON 2019*, Umudike, Nigeria, 2-4 September, 2019, pp. 1-11.